

# Future Developments In Engineering

As engineers gather in New York for the 1960 International IRE Convention, major interest centers on developments now emerging from the laboratory. Here's a look at what lies ahead

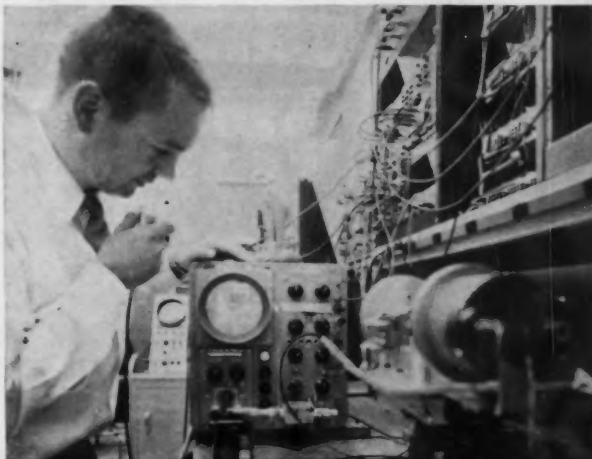
By **THOMAS EMMA**, Associate Editor,  
**MICHAEL F. WOLFF**, Assistant Editor

IN EVERY BRANCH OF today's electronics industry, new developments lie ahead. The scientists, engineers and technicians who shape our future are finding new and better ways to communicate, to solve problems and to expand the horizons of knowledge.

It would be literally impossible to describe each new development that lies ahead. In surveying the immediate practical future, however, certain salient developments emerge. An idea of what lies in the far future may be had by looking at some of these.

**COMPUTERS**—New developments in learning systems, cryogenics, miniaturization and microwave techniques are topics most frequently mentioned in the immediate future of computers.

In the area of learning, such systems as the Perceptron, the Artron and others are coming under



Challenger shows pattern for the spoken words "Tom Franklin" in speech pattern generation experiments at IBM. Work is aimed at determining the unique characteristics in sound.

Bell Labs' engineer submerges specimen of a new ternary semiconductor with liquid nitrogen during a typical materials research experiment. Typical properties being measured are carrier mobility, resistivity and magneto-resistivity.



close scrutiny. The Artron (see Fig. 1), still in the theoretical stage, consists of a semi-randomly connected network of artificial neuron-like decision units and generalized goals operating on the "reward and punishment" system. The Perceptron for which hardware exists is described as a machine able to perceive, recognize and form conclusions.

As indicated in Fig. 1, the Perceptron utilizes binary devices known as response units that are activated by randomly-selected units in the association system. When activated, the response units transmit feedback signals to their associated source sets that tend to multiply the activity rate, resulting in a form of reinforcement.

Work done on self-organizing learning machines has resulted in systems which can play checkers and chess, solve plane geometry problems and solve equa-

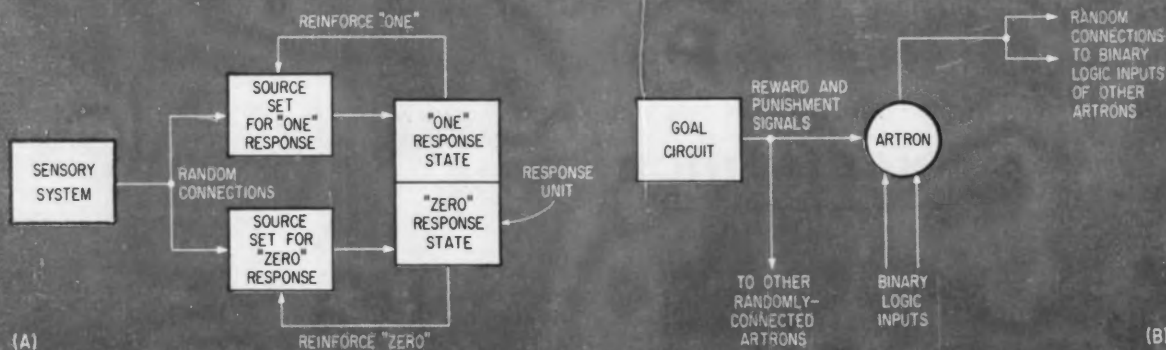


FIG. 1—Block diagrams for Cornell Aeronautical Labs' Perceptron (A) and Melpar's Artron (B) illustrate two approaches to the development of learning machines

tions in symbolic logic. The main advance represented by these systems, in the opinion of most computer men, is that the way has been pointed to means of raising the level of sophistication of computer technology. Final applications, though discussed with caution, will eventually lead to a host of functions ranging from operation of factory production lines to battlefield surveillance and tactics.

**TUNNEL TRIODES**—One line of tunnel diode computer research involves the tunnel triode—a transistor-like structure in which the emitter-base junction is a tunnel diode and the collector-base junction a conventional diode. In a computer application, the triode could be biased so the emitter-base circuit, which exhibits the conventional tunnel diode negative conductance, has two stable states: a low resistance state in the tunnel-current phase and a higher resistance state in the normal diode forward current phase. The former is associated with high collector resistance and the latter with low collector resistance. Thus, the input and output can be separated and the state of the emitter-base tunnel diode determined in the collector circuit.

One area slated for intense consideration will be the possible application of analog computers to functions now performed by digital equipment. There are some computer men who feel that users have been made more aware of digital computers than they have of analog gear. The result, in some cases, has been inefficient use of equipment. An expected result in the near future will be a combining of analog and digital techniques to a greater extent than is now being done.

**COMMUNICATIONS**—Keynote of communications in the next few years will be growth. More traffic handling capability and more methods of communication will be the goal of researchers.

One phase of this will be an experiment slated for this spring. Researchers will send aloft a 100-ft. aluminized balloon which will act as a passive reflector in a one-hop system. The next step in the development of orbiting satellites as a means of com-

munication will be experiments with an active system placed aloft. Researchers consider masers as greatly important to the future of such systems. Present estimates are that masers can operate at about 100 times less power than equivalent vacuum tube equipment.

Microwave systems, both line-of-sight and over-the-horizon will come in for increased attention during the next two years. One development slated for growth is Bell's TH microwave system, able to double the present capacity of common carrier line-of-sight links by the use of newly-designed antennas and ancillary equipment.

Over-the-horizon systems are now going up which will give more channels for military communications in the arctic. In addition, there are expectations that the next few years may see the beginnings of troposcatter systems in Latin America and possibly in certain sections of the Orient.

Single-sideband and double-sideband equipment is expected to see a considerable amount of increase in the near future. A spokesman of one major communications corporation says the "surface is just scratched" in this area. Development of new equipment permitting operation at higher power levels is cited as one important factor that will spur growth in SSB traffic.

In addition to squeezing more work out of existing spectrum space, one hope for the immediate future will be the stretching of the spectrum by utilization of the millimeter-wave region. Researchers have been probing the area above 35,000 Mc for about seven years and have already developed a significant amount of actual hardware. Problems now being attacked in connection with millimeter-wave studies center about development of increased power output. More than one research group feels that the bulk of the power problems are just about solved. Parametric amplifiers are said to show considerable promise in allowing the desired powers to be attained. Mixing and detection systems as well as generators, antennas and receivers now exist which can be used in millimeter-wave transmission.

A most important area of application now seen

for millimeter-wave gear is communication with space vehicles during reentry.

**BROADCASTING**—Engineering developments in commercial broadcasting in the immediate practical future will center around increased station automation. Continued attention will probably center around devices and systems to perform switching functions for program input and output sources. It is likely that a greater amount of instrumentation will find its way into television stations rather than radio stations because of the greater complexities of transmitting video and audio at the same time.

Adding to the need for equipment to perform switching functions rapidly is the continuous rise in the amount of magnetic tape recording that is being used in television. Network stations that handle this taped program fare will require increasing amounts of automatic equipment for inserting local programming in the form of slides, film and live fare into the taped output.

Stereophonic broadcasting, the subject of much recent speculation, will not be making the big breakthrough for some time according to a number of broadcasters interviewed. In terms of engineering, much of the hardware for both transmission and reception is already in existence. The stumbling block, as many see it, will continue to be the absence of hard-core specifications.

Although much experimental work has been done in the use of single sideband in radio broadcasting, it appears unlikely that much will be done in the way of engineering of new equipment for the next 24 months. Pressures both economic and technical to push for development of commercial SSB gear are not strong enough at this time.

From discussion with a number of broadcasters

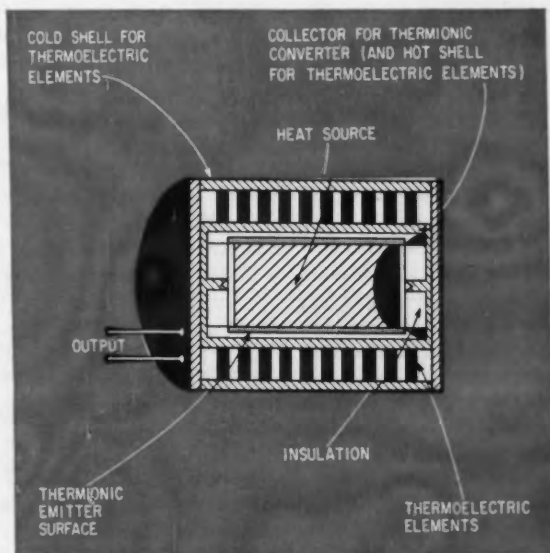
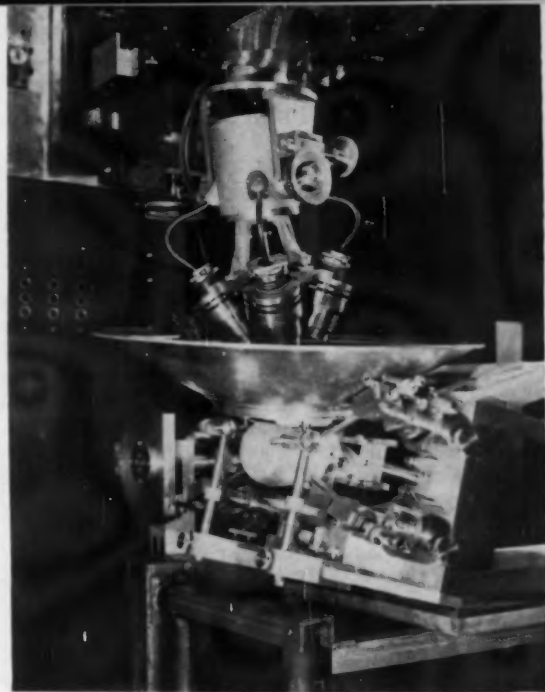


FIG. 2—One design approach to cascaded thermoelectric and thermionic converters being considered at General Instrument is illustrated. Heat source could be nuclear or focused solar energy



Four-beam focusing irradiator is used for ultrasonic neurosurgery studies at Massachusetts General Hospital. Human skull is shown mounted in head holder

both in radio and television, it appears unlikely that any profound changes will be made in commercial broadcasting as a result of the Geneva Conference on frequency allocations. (ELECTRONICS, Feb. 19, 1960, p 33).

**MICROMINIATURIZATION**—Extensive work in the several approaches to microminiaturization will mark the effort in this field during the two years ahead. Microminiature diodes and other minute components will appear in appreciable numbers during this period in engineering prototype equipment. Also, there will be greater use of high-density packaging techniques for standard components using welded interconnections and resins.

Within the next twelve to twenty-four months, *en-bloc* (solid) circuits are expected to show up in such items as digital computers still in the laboratory stage. There, *en-bloc* circuits will be used as flip-flops, AND gates and OR gates. Digital computer 10-Mc logic elements in small transistor cases will most probably be available within a year. Fabrication of these devices will rely on diffusion and deposition techniques.

Researchers at Westinghouse hope to show that their molecular electronics concept for *en-bloc* circuits is feasible for systems applications with the production of a uhf receiver by 1962. Other firms are also active. Major areas that will claim attention during the next few years will be reliability, heat dispersion and integration with tunnel diodes.

One promising approach to microminiaturization is the thin-film technique in which discrete components are deposited on a single wafer and interconnected by evaporated materials. Major research effort in thin-films will be to deposit active elements and improve material handling techniques to allow

greater resolution and lower costs. Some researchers have already reported resolutions of a few hundred angstroms using electron microscope-type techniques.

**DIRECT CONVERSION**—The next two years will see increased progress in the development of devices for converting heat into electric power without the use of moving parts.

For thermoelectric converters, observers anticipate the emergence of special purpose power generators with operating efficiencies of 15 percent. Special devices foreseen include a 100-Kw water-cooled generator with 10-percent efficiency for laboratory demonstration. Also expected are generators ranging from 200 to 500 watts with operating efficiencies of about 6 percent. These will be used in satellite applications.

Achievement of 15-percent efficiencies is predicted on the basis of expected progress in material research. Especially promising are ternary compound semiconductors and transition metal compounds, as well as the solid solution alloys of these substances.

Major efforts of materials-study groups will be attempts to raise operating temperatures and figures of merit. A breakthrough in high-temperature thermoelectrics is not expected within the next two years. Anticipated, however, is a demand for thermionic converters at high temperatures in general, and ranges above 1,500 C in particular.

Demand will most likely bring about significant improvements in thermionic converters during the next two years. Vacuum diode converters with 10 to 15-percent overall efficiencies are expected to be in limited production within the next 24 months. These will have module power ratings of 200 to 500 watts and will be capable of being arranged in series for total outputs as high as 10 Kw.

These improvements will result from extensive materials research aimed at finding collector materials having the lowest possible work function consistent with the emitter chosen and the device lifetime.

One very likely application of vacuum diode converters within the near future will be for space vehicles in which solar energy will provide emitter heat source.

**CESIUM DIODES**—Prototype 100-watt cesium diodes with efficiencies of 15 to 20 percent are expected to be available for such specialized applications as auxiliary power sources for space applications two years from now. Major research effort for this class of device is directed towards the problem of understanding the functions of the plasma in various parts of the converter, and improving production techniques and materials technology. Research is also aimed at finding structural materials that can withstand the corrosive effects of cesium at temperatures as high as 2,300 C. One group of materials being studied in this connection includes such ceramics as zirconium carbide.

One approach to increasing efficiency of direct conversion systems is the cascading of thermoelectric

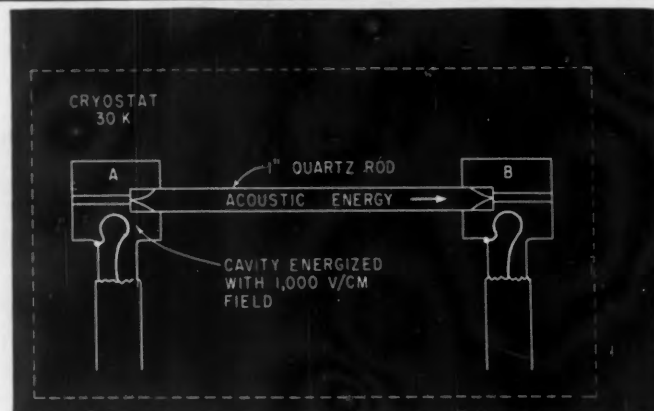


FIG. 3—Acoustic energy of frequencies above 10,000 Mc might be used in a quartz delay line of this type for information storage. Acoustic energy is reconverted to electromagnetic energy in cavity B

and thermionic converters. One such possible combination is shown in Fig. 2. Such a system would use the reject heat from one converter as the source heat for the next.

Magnetohydrodynamic (MHD) power generation appears to be several years distant as a commercial power source. Stationary MHD power generators are large power devices becoming efficient above ten megawatts. Present research in this area centers on cost reduction and increased efficiency.

**THERMOELECTRIC COOLING**—Materials having figures of merit between 4 and 5 are expected to be available within two years. According to industry sources, this means that thermoelectric refrigeration will come near to being as efficient as compressor-type refrigerators. However, the most likely applications of thermoelectric cooling within this period are of the special type, such as cooling infrared detectors, spot-cooling of electronic equipment and military applications.

**LOW-NOISE DEVICES**—With noise figures already to the point where antennas are becoming the limiting elements, low-noise device work during the next two years will turn increasingly to pushing toward higher frequencies, designing gain-stable systems for untrained operators and developing new forms of quantum-mechanical amplifiers.

For masers, the search for new materials, such as emerald, will play a key role in obtaining millimeter-wavelength operation. Another approach being worked on is to generate or amplify very high frequencies on a pulsed basis by converting magnetic field energy, supplied to an inverted spin distribution, into coherent radiation. This technique has been demonstrated by starting with low-frequency operation of a pulsed field maser and extending to the millimeter region by systematically increasing the peak pulsed field.

Continued and important growth is foreseen in the next two years for the optical and infrared masers. These devices are expected to become significant for space communications because they give coherent sources of energy with narrow bandwidths. Working infrared and optical masers for communications and radar-like purposes are expected within two years.

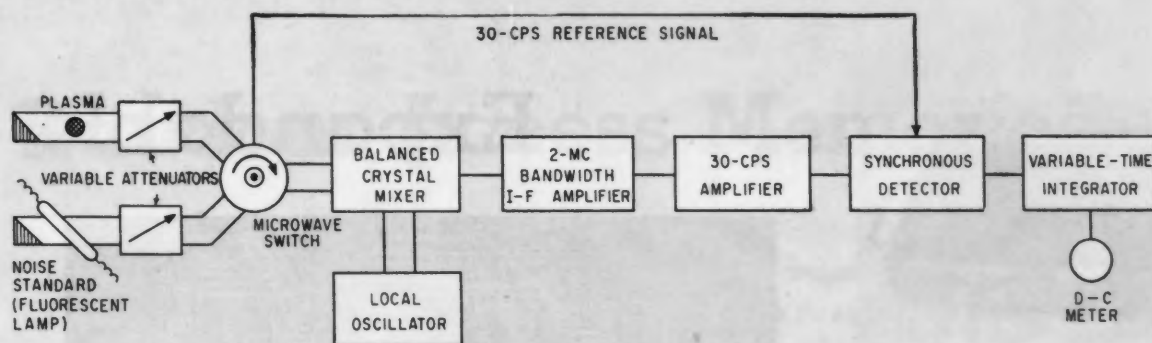


FIG. 4—MIT's S-band radiometer measures noise radiated from plasma at power levels down to  $5 \times 10^{-17}$  watts. Plasma is contained in tube which passes through waveguide in direction perpendicular to direction of propagation and oriented either along or transverse to electric field in the dominant  $TE_{10}$  mode

A wide variety of solids, liquids and gases are being investigated as offering reasonable possibilities for the device material.

Low-noise parametric amplifiers with variable-capacitance diodes will also receive considerable attention and are expected to start appearing in operating systems. The trend will be to use more diodes per amplifier to achieve isolation, pump suppression and self-protection. Along with achieving more sophisticated circuit design, a major effort will be expended in diode materials technology. While some workers predict diffused silicon diodes being widely used in receivers for all frequencies through 16,000 Mc, a lot of work is being devoted to gallium arsenide because of its higher carrier mobility. Proponents of this material expect to have the problems associated with doping and high-temperature processing of gallium arsenide under control within two years.

**ESAKI DIODES**—Although it is possible that tv sets using Esaki tunnel diodes will be in the preliminary circuit design stage two years from now, the major applications for tunnel diodes are more likely to be in industrial and military electronics in this period. Areas most often mentioned as being realizable are communications systems above 3,000 Mc, reactor control circuits and computers. It is in the computer area that tunnel diodes are expected to find the most use during the next two years, with some workers predicting laboratory-model tunnel diode computers with 50-Mc information rates.

Packaging and exploitation of new materials will receive major attention. Gallium arsenide looks promising because of its power handling capability (four times that of germanium diodes in the gigacycle range) and its peak-to-valley current ratio (60 to 1); indium antimonide tunnel diodes have been predicted as possibly leading to millimeter-wavelength amplification.

**ULTRASONICS**—Having proved its value in such applications as cleaning and fatigue testing, the field of ultrasonics is expected to grow even greater.

Further refinement in cleaning and testing techniques as well as welding in specialized application is seen to be a certain development. In addition, increasing attention will be paid to development of

new devices and in study of hypersonics, (behavior of sound above 1,000 Mc.).

In hypersonics, one phenomenon that will receive much attention centers around evidence that sound at 30 K can be transmitted with practically no attenuation. One possibility suggested by this is the use of high-frequency delay lines to store large amounts of information in a limited amount of space. Researchers say this may point the way to computer storage applications. One possibility is a quartz rod delay line as shown in Fig. 3. In such a device 10,000 bits of information can be stored at 10,000 Mc.

Present research programs are aiming for 35,000 Mc with hopes of eventually reaching 100,000 Mc.

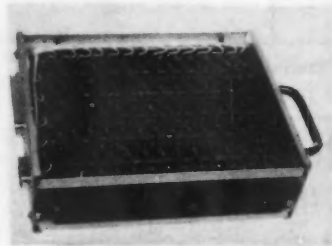
**PLASMA PHYSICS**—Research into the properties of plasma will play an increasingly important role in such areas as controlled thermonuclear fusion, ionospheric communication, thermionic converters and telecommunications during space vehicle reentry. In addition, however, considerable work is underway in the use of plasmas to develop new microwave circuitry and generate extremely high power at very short wavelengths. Judging from current research results, some researchers expect basic research in this field to bear fruit in two years.

Among techniques developed for plasma research is microwave measurement of electron temperature, one of the fundamental parameters of interest. An S-band radiometer that calculates electron temperature by measuring the noise radiated by the plasma is shown in Fig. 4.

**MEDICAL ELECTRONICS**—Although a considerable number of devices have been provided which permit medical tasks to be performed electronically, doctors see the next few years as being marked for increased growth in understanding. Based on past accomplishments by both medical men and engineers, it appears that there is more awareness on the part of each of the way they can be of mutual aid in research and development programs.

Regarding present equipment, a vital need seen for the near future is research that will bring down costs and make today's devices available to a greater number of users.

# Expandable



Memory package is composed of spaced stack of five core planes, a top and bottom shield plane, and a top and bottom diode board

FIG. 1—In this expandable memory, a variable number of memory packages may be used

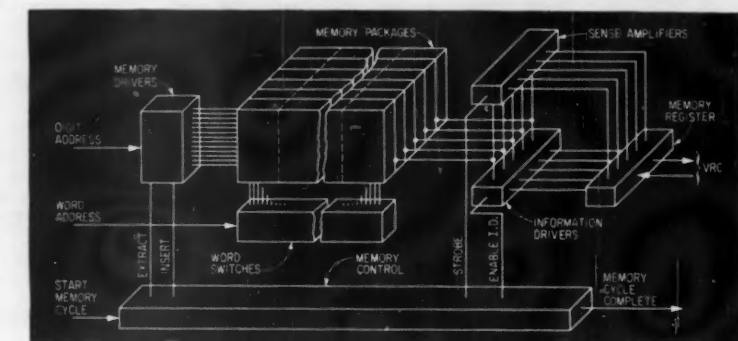
**P**LUG-IN MEMORY packages form the basis of an expandable solid-state linear select memory used in the Burroughs B-251 Visible Record Computer (VRC). This computer, which operates over a wide range of temperature and supply voltages, is a small digital computer designed for banking and similar business applications.

Input is provided by a sorter-reader which is capable of high-speed sorting and reading of checks and other items using the magnetic-ink character recognition system of the American Bankers Association. Output is provided by an integrated, automatic ledger and journal posting handler.

Memory for the VRC uses magnetic cores operated in an expandable linear select random access array. This memory, which is variable in size, is designed to permit a wide latitude in component tolerances.

## Memory Description

Block diagram of the expandable memory is shown in Fig. 1. Each memory package has 10 groups of addresses (words) shown being addressed from the word switches at the bottom of the memory block. Each word has 13 addresses (digits) which are selected by the memory drivers shown at the left of the memory packages, and each address has a capacity of five bits, one in each of the five bit planes. Word switches are associated with individual memory packages; consequently, additional word switches



must be added when memory packages are added. The memory drivers are connected to all packages in parallel and the bit planes of all packages are connected in series. The memory control circuits control the operation of the memory upon receipt of the start pulse and then return a *complete* pulse to the computer at the conclusion of the extract-insert cycle.

With the linear select memory configuration, as will be explained, the disturb currents are only one third of the full switching current; thus, the memory uses less critical currents and components, and operates over a wide temperature range. A typical memory address, as in Fig. 2, is reached by first selecting one of the bilateral word switches. It is normally energized on a d-c basis and permits the addressing of all digits in the selected word. A

memory driver (extract and insert) is then selected by a digit address from the computer. The digits are generally addressed in sequence within each word. At the arrival of the start pulse, the extract timing pulse passes through the one opened digit gate and causes the extract driver to conduct the full switching current. The sense amplifiers receive the switching voltage of the cores which were storing *ONE*'s by means of the bit plane winding. A strobe pulse permits the output of the sense amplifiers to transfer the information to the memory register. The sense amplifier gate also has an erase input to prevent the old information from reaching the memory register while new information is being inserted. The information driver enabling pulse immediately turns on the information drivers, either  $+\frac{1}{3}$  or  $-\frac{1}{3}$  full

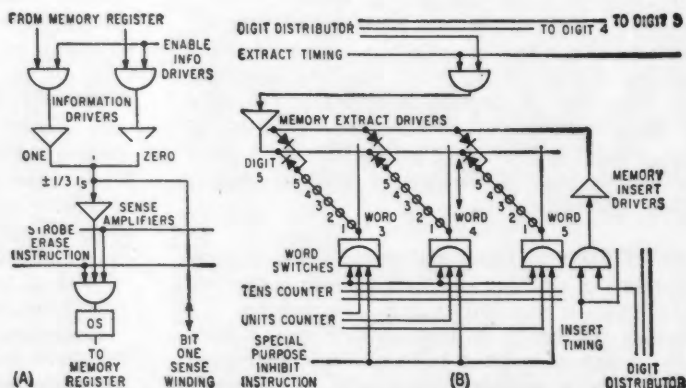


FIG. 2—Shown here in (A) and (B) are basic elements of a typical memory address

# Random Access Memories

These expandable solid-state memories operate in an ambient temperature of from 15 to 55 C and require no better than plus or minus three percent supplies. Plug-in feature provides unusual economy

By **GEORGE E. LUND**, Development Engineer, and **DONALD R. FAULIS**, Associate Development Engineer, Burroughs Research Center, Paoli, Penna.

switching current depending on the state of the memory register. The insert memory driver is then caused to conduct a  $\frac{1}{2}$  switching current which, in combination with the mmf produced by the information drivers, produces either a full switching mmf or an inconsequential  $\frac{1}{2}$  switching mmf. A complete pulse is then returned to the parent system.

Since speed is not a problem, the minimum memory recycle time is made approximately 80  $\mu$ s which has the advantage of low dissipation and reduced recovery time problems. The memory access time is approximately 10  $\mu$ s.

## Memory Package

The memory package is composed of a spaced stack of five core planes, a top and bottom shield plane, and a top and bottom diode board. The

cores are loosely laminated between sheets of paper base phenolic laminate on which a part of the series-connected bit plane winding is printed. The discontinuous printed pieces of the bit winding are connected by means of staples which pass from one printed pad through a core to the back of the board and then through a second core to the next printed pad. Short leads are used from the corner of the core planes to the small connector, which is adjacent. Transverse wires are inserted through each stack of five cores and soldered to the diode boards at either end. Digit address wires within each word are connected longitudinally by the printed circuit on one diode board while the diodes for that word group are mounted on the opposite diode board. The pattern is alternated so that the same diode board can be

used for either side. Digit extract and insert lines are printed on the under-side of the diode boards and run from side to side. Word and digit leads terminate on the large connector and are dressed along the bottom and edges of the package opposite to the side on which the bit plane windings are connected.

## Addressing Circuits

A memory address is chosen by the computer, which selects a word by means of the word switches and then selects a digit through the digit's memory current driver.

The word switch, Fig. 3, which closes the selected word circuit, is basically a bilateral switch. A symmetrical transistor, RCA TA1703C, is used; two additional transistors are required in the circuit, a 2N269 buffer driver and a 2N269 input decoding gate. A *units* and *tens* input

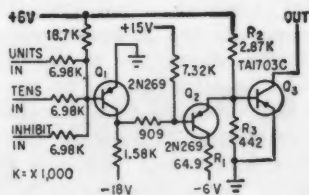
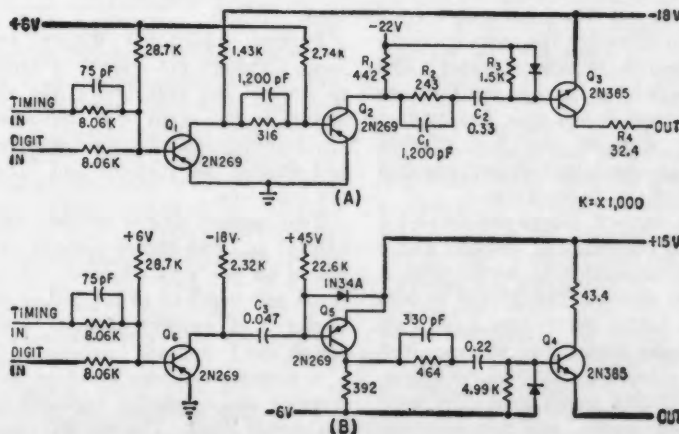


FIG. 3—Word switch, which closes the selected word circuit, is basically a bilateral switch

FIG. 4—Memory driver consists of an extract driver circuit (A), which supplies current to extract information from the memory, and an insert driver circuit (B), which supplies current to insert information into the memory



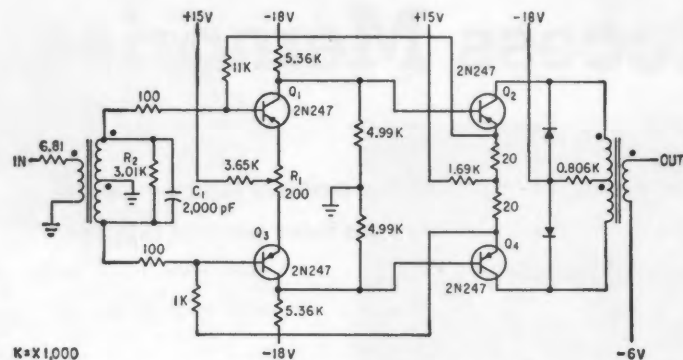


FIG. 5—Minimum input from the cores to this sense amplifier is 30 mv

is used to select a particular word. The third input to the gate is for a special purpose inhibit instruction. A word switch must be selected at least 10  $\mu$ s before the memory start pulse is received. This presaturates  $Q_3$  in preparation for the memory driver currents. The transistor requires a heat sink to keep its junction temperature below 75 C with a 55 C ambient at maximum dissipation. Collector-to-emitter voltage is less than  $\pm 0.3$ v when passing the full 500-ma memory current. Divider resistors  $R_2$  and  $R_3$  are used to insure that the TA1703C is biased OFF in the unselected circuits;  $R_1$  assures bottoming of  $Q_3$  when the circuit is selected. Worst case design approach is used throughout.

Four of these circuits are placed on one 4½ by 7-inch printed circuit card. Twenty-five cards are required to accommodate the full 100-word memory.

The memory driver (Fig. 4) consists of two circuits, one to supply current to extract information from the memory and the other to supply current to insert information into the memory. These currents switch or help to switch the memory cores to opposite remanent states. The full switching current for the core being used is 500 ma. The extract driver supplies the full current whereas the insert driver supplies but ⅓ of the full current.

The current source consists of a current determining resistor and a 2N385 transistor in series with a voltage source. The 2N385 is bottomed during driver operation. Two additional transistors are required in the circuit, a 2N269 buffer driver and a 2N269 input gate. The gate has two inputs, one for selection

of the memory driver (digit) and one for timing the driver in the memory cycle. Extract and insert circuits are very similar, the difference being the direction of current flow and the resulting bias and voltages required.

In Fig. 4,  $R_2$  is the base current determining resistor;  $R_1$  and  $R_3$  are used to supply reverse base current to quickly turn off  $Q_3$ . Capacitor  $C_2$  is used in the circuit as an a-c coupling to insure that  $Q_3$  cannot be inadvertently held on continuously, thereby preventing over-dissipation of  $Q_3$  and  $R_1$ .  $C_2$  discharges through  $R_1$ ,  $R_2$ , and  $R_3$ . Capacitor  $C_1$  is a speed-up capacitor shunting  $R_2$ , which reduces  $Q_3$  base delay and rise time. One small difference in the insert circuit is the a-c coupling  $C_1$  which is used instead of a simple resistance circuit to couple the first and second stages. This was used to accommodate the power supplies available and a standard input gate which accepts a -7v to ground signal from the computer. The IN34A in Fig. 4B is used to hold  $Q_3$  normally off by applying a positive d-c bias.

Several additional diodes are used, although not shown, in order to protect the transistors and resistors in the event of a failure of any combination of supply voltages and during the turn-ON and turn-OFF intervals.

Two memory driver circuits, two extract and two insert circuits are placed on one printed card. Seven cards are required to accommodate 13 digits of memory capacity with one driver for spare.

A memory address contains five memory cores, one for each bit in the stored digit. The bit informa-

tion is handled in five parallel channels. Each channel contains the memory cores of all addresses for that bit, a sense amplifier to amplify the core outputs and an information driver to insert ZERO or ONE information in the addressed core.

### Sense Amplifier

The minimum sense amplifier input from the cores is 30 mv. The minimum output pulse is 6 v. The amplifier is balanced to reduce common mode noise and reduce the pulse repetition rate sensitivity which would have resulted by the use of RC decoupling circuits. The sense amplifier uses two stages of 2N247 transistors as shown in Fig. 5. Resistor  $R_1$  is required to achieve a balance in the amplifier with initial variations in the components.

Noise is a major problem in the design of the sense amplifier. The information driver, which is physically connected to the same channel wiring as the sense amplifier, contributes the largest portion of noise. The noise is discriminated against, in time, by a strobe gate at the output of the sense amplifier.

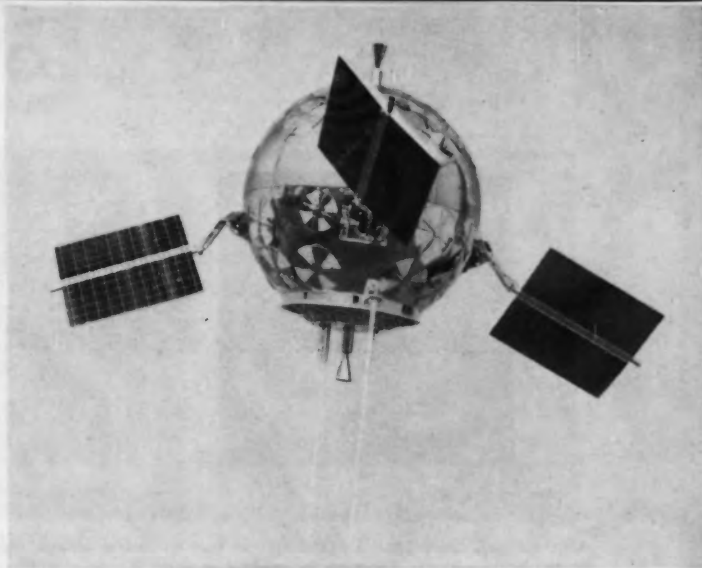
Noise is also produced by the capacitive coupling of the sense winding and the memory extract driver. This situation is aggravated by the long length of the sense winding necessitated by the plug-in type memory packages. An RC filter ( $R_2$ ,  $C_1$ ) is used at the input of the sense amplifier to help reduce this noise.

The amplifier has negative feedback in each emitter circuit and overall feedback for gain stability with a range of components and temperature variations.

The amplified signal from the memory sets the memory register for buffer storage, by means of a one-shot multivibrator. The register selects the ZERO or ONE circuit of the information driver when inserting the information back into the memory. The information driver is very similar to the memory driver, except that it drives plus or minus ⅓ of the full switching current. As explained previously, the insert memory driver supplies ⅓ of the full switching current; therefore, the information mmf is added to or subtracted from the insert mmf to insert a ZERO or ONE.



THE FRONT COVER—Once in orbit, Able space probe appears as shown with solar cell-bearing paddles extended.



# Solar-Cell Power Supplies For Satellites

For reliability in the space environment, silicon solar cells are proving their worth. In this article, basic design considerations are treated with details of their applications to the Able-4 Atlas space probes

By ROY M. ACKER, ROBERT P. LIPKIS, RAYMOND S. MILLER and PAUL C. ROBISON,  
Space Technology Laboratories, Inc., Los Angeles, Calif.

**S**PACE PROBE power sources that operate unattended for considerable lengths of time have been necessary for some time, and the sun has been obvious as a convenient source of power. Because of weight limitations in space vehicles,

devices which convert solar radiation directly into electrical power have immediate appeal. The three space vehicles in the NASA Able-3 and -4 programs have all used a system for electrical power supply in the payload which has involved special adaptations and designs.

Basically, these vehicles have relied on silicon solar cells cemented on four paddles extended out from the surface of the vehicle and operating in conjunction with storage batteries within the vehicle. Although there are minor differences among the three vehicles, the basic design for the power supply has been the same throughout. One of the goals of the design, in fact, was to achieve a sufficiently versatile system so that it could apply equally well to the three missions: the large elliptical earth satellite orbit of Able-3, the lunar satellite orbit of Able-4 Atlas, and the heliocentric

orbit of Able-4 Thor. The application of the system to a particular vehicle, the Able-4 Atlas space probe, will be described.

Because of its relatively high efficiency and its availability, the silicon photovoltaic cell was chosen as the device for conversion of sunlight to electricity in the power supplies for the Able space probes.

Once silicon solar cells in conjunction with storage batteries had been chosen as the power source, several design problems had to be met. It was clear almost from the first conception of the vehicle that the cells would have to be mounted externally to the shells of the payloads. To cover any significant fraction of the payload shell with solar cells would complicate the temperature control problem of the payload, and to obtain the required 30 watts of power for the payload a greater area for solar cells was needed than

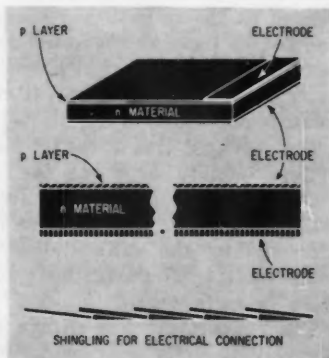


FIG. 1—Construction details of cells and method of connecting

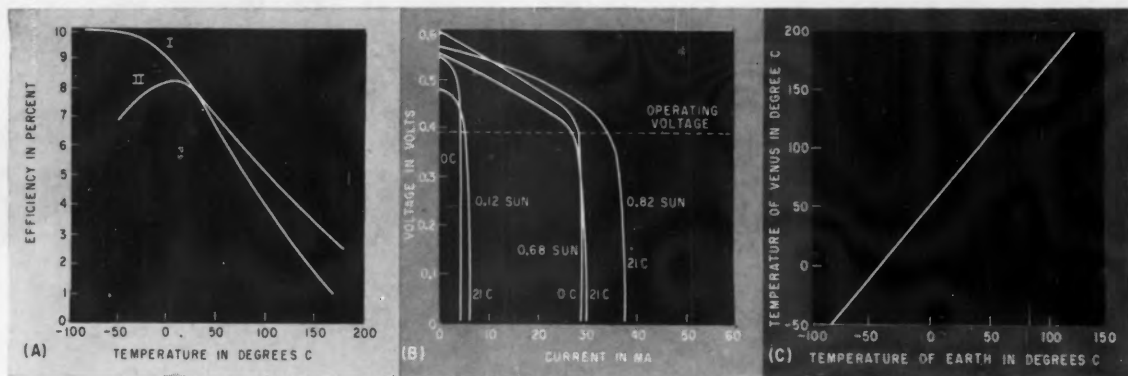


FIG. 2—Temperature effect on efficiency (A) and an current-voltage characteristics of 8 per cent silican cells (B). Expected temperature at Venus is compared to measured temperature at earth (C)

the shells conveniently supplied. Hence, it was decided to use paddles extending radially from the equator of the vehicle, with the solar cells cemented to their surfaces.

The geometry of a silicon cell is illustrated in Fig. 1. Length and width of the unit are limited by the size of the crystal from which the cell is cut and by the need for high collection efficiency at the electrodes. Thickness should be small to minimize resistance in the  $n$  material. This is not a design problem since resistance can be kept below 0.25 ohm with thicknesses in the range of 0.1 to 0.5 cm. A more critical dimension is the thickness of the  $p$  layer. Since the large majority of hole-electron pairs produced by sunlight are created within one micron of the surface, two contradictory demands are made on the  $p$  layer: a thick layer reduces its resistance but a thin layer reduces the loss by recombination since the volume through which the freed electron must move without encountering a hole is thereby reduced. For cells of the size used in the Able programs (1 by 2 cm) optimum  $p$ -layer thickness is approximately one micron.

#### Cell Construction

In very general terms, a silicon solar cell is constructed in three steps. The crystal ingot is carefully grown in a melt into which arsenic is introduced as an impurity. Individual cells are then sliced from this ingot and shaped to the desired thickness. These cells are then diffused with boron from the gas of a boron compound and the boron impregnation removed from

the bottom and all sides of the cells. The arsenic impurity serves therefore to define the  $n$  material and the boron the  $p$  layer for the  $p$ - $n$  junction.

#### Temperature Dependence

Silicon solar cells suffer a loss of efficiency with increased temperature at the rate of about 0.6 percent per degree C above room temperature. Efficiency increases with lower temperatures, but the rate of increase is effectively zero as the temperature approaches about  $-100$  C. Typical curves of efficiency plotted as a function of temperature are given in Fig. 2A; in curve I the load impedance is optimized for each temperature, while in curve II the load impedance is optimized at a fixed temperature (25 C).

It is known empirically that the open-circuit voltage decreases and the open-circuit current increases nearly linearly with increasing temperature. The short-circuit current, however, rises at a rate of only about 0.07 percent per degree C, a rate small enough to be ignored in practical applications. Figure 2B illustrates these effects by plotting voltage-current curves for two temperatures at different light intensities. These curves show that current is nearly independent of voltage just below the knee of the  $I$ - $V$  curve.

The temperature of silicon cells mounted on a vehicle surface depends on several factors: radiation both to and from the cells and within the payload shell; conduction between payload components and parts of the non-isothermal shell; and power dissipation, both con-

tinuous and intermittent, within the payload. With the cells mounted on paddles, this thermal isolation from the payload is sufficient so that the energy balance at the cells can be closely approximated by considering only the effects of radiation.

By careful design to reduce the conduction loss through the paddle, the temperature of the solar cells on the back face can be made to approximate the temperature of the cells on the illuminated face so that the back face will radiate at the same temperature as the front. The temperature,  $T$ , of the cells can then be closely approximated by the expression

$$T^4 = \frac{\alpha G A_p}{\epsilon \sigma 2A_s}$$

where  $\alpha$  is the absorptivity of the material integrated over the out-of-the-atmosphere solar spectrum, and modified for this purpose to be the fraction of incident solar energy absorbed but not converted to electrical power for the material,  $\epsilon$  is the emissivity of the surface material defined as the ratio of the energy emitted by the material at its own temperature to that which would be emitted by a black body at the same temperature,  $G$  is the solar energy per unit area at the location of the satellite,  $\sigma$  is the Stefan-Boltzmann constant,  $T$  is the absolute temperature,  $A_p$  is the area intercepted by the sun's radiation, integrated for a rotating body and  $A_s$  is the surface area.

The temperature will change, of course, with  $G$ , the solar energy per unit area. The sun's intensity at the orbit of Venus (0.72 astronomi-

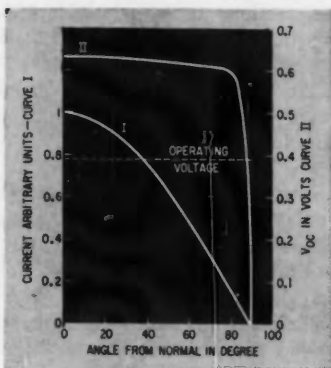


FIG. 3—Electrical characteristics are for cells rated at 8 percent efficiency at 0C

cal unit from the sun), for example, is about 1.9 times that of the earth. Thus on a trajectory reaching Venus the temperatures attained as compared with the temperatures near the earth are as shown in Fig. 2C. A solar cell power conversion system which would operate satisfactorily at the orbit of the earth may reach sufficiently high temperatures at the orbit of Venus to cease functioning unless some active cooling is employed or unless the cells are made to operate at a temperature sufficiently low at the earth so that they will still perform satisfactorily at the orbit of Venus.

#### Low Ratio Desired

It is clear from the previous expression that a low value of the ratio  $\alpha/\epsilon$  is desired to achieve a low cell temperature. Unfortunately, this ratio for a silicon solar cell is high; the absorptivity,  $\alpha$ , is about 0.94 and the emissivity,  $\epsilon$ , is only about 0.31 because silicon is semi-transparent in the infrared and the emissivity of the upper surface of the metallic bottom layer of the cell is low. Emissivity can be raised by cementing glass plates to the silicon cell face or by spraying or vacuum-depositing suitable optical coatings. Effective absorptivity can be lowered by applying an interference filter which reflects a portion of the solar spectrum outside the region of electrical sensitivity of the cell, 0.4 to 1.1 microns. In addition, the temperature of the cells can be further reduced by coating the paddle area that is not active cell area with a material with a low ratio of  $\alpha/\epsilon$ .

It is not necessarily advisable,

however, to attempt to achieve the lowest possible equilibrium temperature for the silicon solar cells, since the design of the solar cell array tends to permit a very rapid temperature drop when the payload is in eclipse. Good design will permit the cell-glass-cement assembly to withstand quite low temperatures but a point is reached where internal stress cracks the cell itself. Temperature decrease during eclipse can be reduced by increasing the weight of the array and by decreasing the over-all effective emissivity of the array, both of which, however, compromise other aspects of the design. For the Able vehicles, the trajectories and orbits are carefully planned to minimize eclipse time and delay the onset of long eclipses. In an eclipse lasting an hour, the temperature of the cells will drop to  $-165$  F. Silicon cells can survive this temperature but longer eclipses could cause damage.

#### Power Output

The solar radiant power density at sea level on a clear day with the sun at the zenith is about 100  $\text{mw}/\text{cm}^2$ . Silicon cell power units having an output under these conditions of 8 or 9  $\text{mw}/\text{cm}^2$  have been constructed, giving efficiencies of approximately 8 percent. Outside the atmosphere of the earth, the power from the sun is about 1.4 times that on the surface of the earth. However, much of the sun's energy absorbed by the atmosphere is in the ultraviolet and violet wavelengths, wavelengths which are almost unusable in solar cells because of reflection and the fact that the excess energy in each quantum serves only to heat the cell. Thus the power density when atmospheric absorption is no longer a factor is about 1.2 of that on the surface of the earth, or 120  $\text{mw}/\text{cm}^2$ . Consequently on space vehicles in vacuum near the earth, cells of 8-percent efficiency at normal inci-

dence to sunlight can generate about 10  $\text{mw}/\text{cm}^2$ .

In general, the power from the solar cells charges storage batteries, or storage batteries regulate the voltage. Thus, the operating voltage of the solar cell is that of the battery plus the voltage across the diode used to isolate the strings of cells from each other. The isolating diode is required since the impedance opposite to the direction of current is very low when a string is in shadow.

The number of cells in series must be carefully selected so that the open circuit voltage of the string of cells is greater than the operating voltage imposed by the battery, assuring that the battery will be charged whenever the current is not negligible. At the same time the operating voltage must not be far below the open-circuit voltage or near-maximum power will not be realized. The importance of having a slow variation of open-circuit voltage with light intensity is thus clear. These requisites are made clear by Fig. 3, which shows the current output of a cell and the open-circuit voltage per cell as a function of the angle of incidence of sunlight. As long as the open-circuit voltage is greater than the operating voltage, the power output is the product of operating voltage and current.

#### Configuration

Under the actual operating conditions of a vehicle in space, the specific arrangement of the solar cells defines in large measure the actual power available to the vehicle. If the configuration places all available solar cells in a plane perpendicular to the normal incidence of sunlight, maximum power will be provided, assuming that the temperature is kept sufficiently low. The attitude of the vehicle with respect to the sun is constantly changing.

As a result, unless an active sun-seeking attitude control system is operating on the solar cell configuration, the angle of incidence on a single-plane configuration will reach zero at some point in a trajectory. Active attitude control systems would have necessitated additional weight and complexity that were not possible in the Able-3, -4

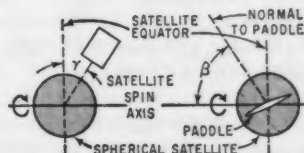


FIG. 4—Angles affecting projected area are defined

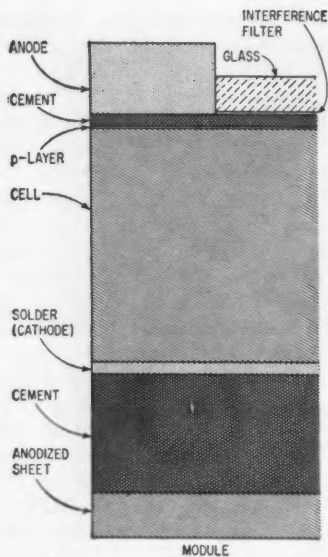


FIG. 5—Cross section (to scale) of solar cell shows relative thickness of layers

programs, and, so far as possible, continuous operation of the power source is needed. A configuration which is relatively insensitive to vehicle attitude and which, except for total eclipse of the vehicle, will continue to provide power to the vehicle is required.

For a spin-stabilized vehicle (as are all three Able space probes) it is convenient to consider the average projected area as a function of the sun's angle of incidence to the spin axis. When the cells are mounted on paddles, the problem is exceedingly difficult to analyze, for the shadowing of paddle on paddles and vehicle upon paddle must be considered. However, it can be shown that the projected area of the paddles as a function of the orientation spin axis with respect to the sun can be defined in terms of two angles, as shown in Fig. 4.

#### Able-4 Design

The power conversion system in an Able space probe must withstand several types of loads and must operate within certain limitations. During launch it must survive strong acceleration and vibration loads. The paddles must erect, latch firmly into place and begin to operate in a period of one second. The system must withstand the centrifugal loads created by a spin rate of nearly 3 rps. After spin-up

and erection, it must withstand a third-stage acceleration and vibration with the paddles erected. After surviving these loads it must operate reliably and effectively for months.

The basic unit in the solar power conversion system in the Able-4 Atlas payload is a strip of five boron-diffused silicon solar cells measuring 1.78 by 0.79 inches and manufactured by Hoffman Electronics. The five cells are electrically connected by shingling, as illustrated in Fig. 1. Each strip exposes an area of 1.347 square inches or 8.69 square centimeters.

In the three Able vehicles, 0.003-inch glass plates are cemented individually to each cell, using a highly transparent cement and taking care to avoid an air or vacuum space between the glass and the silicon cell, thus preventing the temperature rise that would occur as the result of the greenhouse effect. An ultraviolet interference filter, centered at a wavelength of 0.49 micron, protects the cement from degradation by ultraviolet radiation and at the same time aids in temperature reduction by eliminating the energy in a portion of the solar spectrum. Further reduction could be achieved by reflecting the near infrared (1.1 to about 3 microns) but this was not done for the Able vehicles. A cross section of the layers in the solar cell is shown in Fig. 5. The wavelength properties of the incident solar radiation, rejected radiation, and converted radiation in the cell are shown in Fig. 6.

The strips are connected in series, as shown in Fig. 7, on the anodized outer surface of both sides of a tapered block of honeycomb aluminum. The epoxy glue used serves also to insure insulation from the aluminum should the anodized layer become scratched. Ten of these strips form a module, with a maximum weight of about 90 grams. Honeycomb aluminum meets the three requirements of strength, light weight, and good heat transfer characteristics. Subdividing the structure of the paddles into modules allowed for more efficient handling of the paddle. If the paddle were a single indivisible unit, damage to a cell after its inclusion on

the paddles would necessitate removing the cell and very possibly damaging the honeycomb beneath it. In that case the whole paddle would have to be replaced rather than just a module.

The modules are attached to a central tube with 11 modules extending to each side, separated by a distance of 0.2 inch to prevent the possibility of mutual damage during vibration or deflection under load. The tube extends three inches beyond the last module to permit attachment and support during first and second stage firing. With 22 modules to a paddle, 2,200 solar cells are carried on each paddle, 1,100 facing to each side. Thus, 8,800 cells are included in the system.

The paddles are bolted to the four arms on the payload at an angle rotated counterclockwise 33 degrees on the axis of the paddle. In the erected position the paddles form an angle of 60 degrees with respect to the payload's equator (as defined by the spin axis). The arms are paired such that two extend up from the plane of the equator at an angle of 22.5 degrees and two extend down at the same angle. (The 60- and 22.5-degree angles are the  $\beta$  and  $\gamma$  defined in Fig. 4.) The configuration of the paddles established by these angles results in the equivalent of 25 percent of the cells normally oriented to the sun at all times. This configuration results in a projected area which varies no more than about 10 percent regardless of the sun's position. In arriving at the angle of 22.5 degrees a compromise had to be

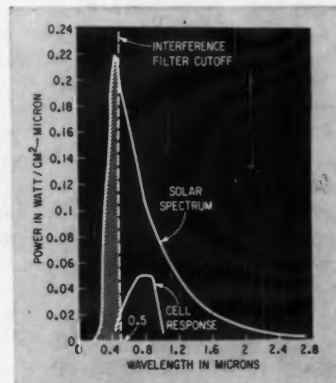


FIG. 6—Power as a function of wavelength for solar spectrum and solar cell response above earth's atmosphere

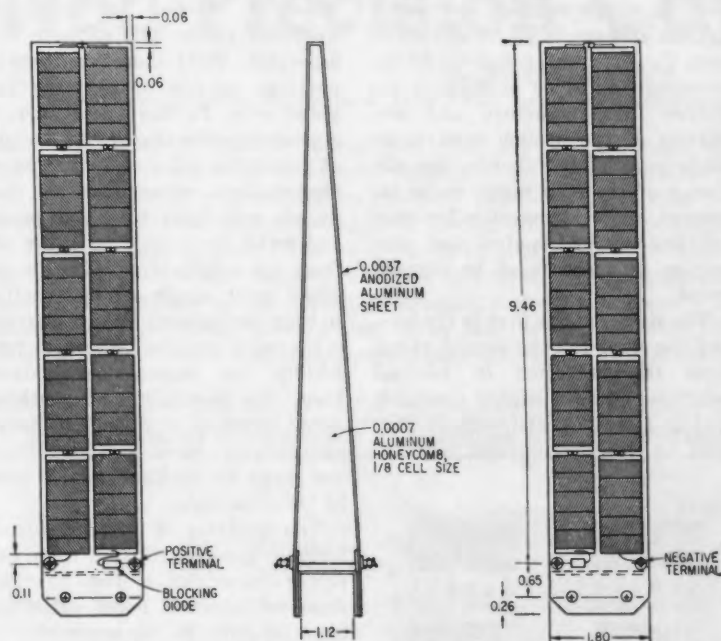


FIG. 7—Dimensions of solar cell module shown in inches. Use of modules simplifies problem of replacing damaged cells

reached between maximum exposure for the cells and stability of the spin axis. Placing the paddles alternately 45 degrees up and 45 degrees down would have produced minimum shadowing of paddle on paddle but would have had the effect of creating equal moments of inertia about two axes of the payload, thus creating the danger of wobble after spin-up.

During launch the paddles are folded vertically in a symmetrical fashion about the Stage 3-4 connecting structure. The tips of the paddles rest in sponge rubber on brackets mounted on the interstage structure and are held in place by a prestretched dacron cord encompassing all four paddles. The paddles are held down against torsion-spring tension at the hinges. When the cord is released, the torque of 19 inch-pounds applied by these steel springs raises the paddles. A separate spring-loaded cam in the arm mechanism locks the paddles in place.

The release and erection mechanism is activated during the coast period before spin-up by an explosive cutter through which the cord is threaded. A timer in the second stage ignites this cutter at the proper moment, to drive a knife-

edge piston through the cord, severing the cord and releasing the paddles.

It is important that the paddles erect at this moment. To permit their erection during first or second stage burning would have required very heavy springs on the paddles to overcome the g-loading imposed by the acceleration. To erect after spin-up, the initial force of which is large, would have imposed a contradictory difficulty, because of too much erection force on the paddles. The centrifugal force created by spin would swing the paddles out with damaging force at latch unless fluid dampers or some form of plastic impact were incorporated. It is essential that the paddles erect to an accurate position to insure dynamic balance within close limits.

#### Electrical Design

With this configuration in orbit about the moon a nominal constant charge current of 1.6 amperes (about 30 watts) could be provided by the paddles. Of this current, approximately 0.85 ampere is needed for the constantly operating electronics in the sensing and recording equipment associated with the scientific experiments. Thus 0.75 ampere is available to charge stor-



Paddles are shown folded back, as they will be during launch

age batteries. These batteries consist of two packs of 14 nickel-cadmium cells each, attached in series. When the 5-watt transmitter in the vehicle is operating, it draws about 2.8 amperes from the system, and therefore during its operation the net drain on the batteries is about 2 amperes.

At this rate the batteries require approximately four hours for discharge as compared to 12 hours for maximum charge. Since complete discharge of the batteries is not desirable, the charge-discharge rates must be carefully watched during flight to try to prevent the voltage from dropping below 17.5 volts. Moreover, an emergency under-voltage cutout is included which automatically turns off the transmitter should battery voltage drop to 15.5 volts. The exact duty cycle is chosen after the vehicle is in flight, on the basis of the telemetered charge current and payload temperature.

Consideration must be given to control of the temperature of the batteries, since their efficiency decreases at a rate of approximately one percent for every 4 degrees F that the temperature increases or decreases in the neighborhood of the optimum of about 70 F. The

active control system incorporated in the design of the Able-4 Atlas served therefore, among other things, to keep battery temperatures within the proper range.

A simplified block diagram of the power supply system is shown in Fig. 8. The switches which activate the solar cell power conversion system are closed when the paddles swing into place. Blocking diodes separate the charge current from the discharge current and isolate solar cell strips when they are shadowed.

### Operation

At launch the batteries are maximally charged, and thus the operation of the transmitter during the immediate postlaunch period imposes no hardship on the power system. However, once initial tracking has established an accurate trajectory and initial telemetry has provided data on paddle activation, charge current, and payload and paddle temperatures, it is necessary to plan transmission times from the vehicles so that the system will not be overloaded.

One payload transmitter can be operated about 30 percent of the time, but the exact duty cycle must be determined after special experiments have been performed with specific battery charge and discharge cycles, and measurements have been made of transmitter temperatures. When fully charged, the batteries in the payload can operate a 5-watt transmitter for slightly more than three hours. By that time, however, the battery voltage is reduced to a level which actuates the undervoltage control, automatically turning off the transmitter and performing the other functions that a ground *Transmitter Off* command would cause.

The Space Navigation Center (Span) at Space Technology Laboratories controls this duty cycle.

### Future Developments

The Able-3 earth satellite (Explorer VI), launched in August 1959, carries a solar cell power conversion system very similar to the one described here. The system has operated satisfactorily. The conclusion, then, is that the general application to power supplies in space

vehicles of this solar cell conversion system appears to be an acceptable one. However, three avenues of improvement must be pursued in the future. The structure and mechanics of the system need to be made completely reliable, the efficiency of the cells needs to be increased, and new materials for solar cell temperature control and protection in space must be investigated.

The need for the first is obvious, and the need for the second stems from the reduction in payload weight—always a highly desirable goal in a space vehicle—made possible by the concomitant require

of value. Surface treatment can presently reduce this value to 7 or 8 percent. Work should continue on coatings capable of reducing this value even further. Moreover, it appears possible that the technology of preparing solar cells can reduce electron-hole recombinations that do not contribute to usable power and make the transition in the cell from one conductivity type to another more nearly a step junction so that the forward leakage current in the cell is reduced. A further possibility for improvement stems from the possibility of stacking semiconductors of differing energy gaps in such a manner as to increase the range of sunlight energy used by the solar cells.

The problem of protection and temperature control of a solar cell power conversion system has two areas of interest. First, attention must be given to the prevention of damage to the system during long periods of eclipse. Obviously it will be impossible to keep eclipse times to periods of an hour or less on all future space vehicles, and hence procedures for assuring that the system can survive long eclipses must be devised.

Second is the problem of preserving the radiation balance of the various surfaces involved in the conversion system. Long exposure of these to the unfamiliar but doubtlessly destructive stresses of the space environment may very likely change the surface optical properties and degrade the operation of the system. In this environment molecular bonds are broken and glass is darkened by ultraviolet and even more penetrating radiations; hard radiation can damage the electrical performance of the cells; materials sublime and evaporate significantly over long intervals of flight in the hard vacuum; stray atoms and molecules cause sputtering of the surface; and micrometeorites pit and erode the surface, particularly glass coatings on cells, and may partially cover the surface with the debris of the impacting particles. The combined effects of these stresses may serve to enhance each other. All of these changes in the surface are reflected in changes in the radiation properties of the surface material.

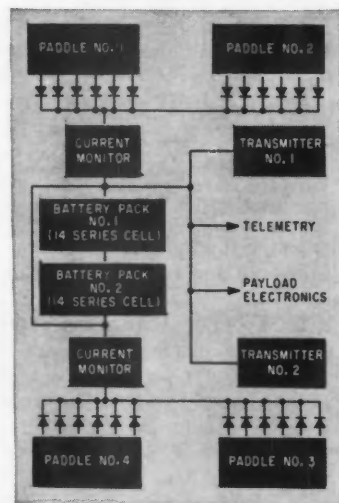


FIG. 8—Transmitter and battery-charging cycles are controlled from ground

ment for fewer cells. The third need stems from the fact that as space exploration becomes more ambitious, with interplanetary ranges and lifetimes of several years desirable, present  $\alpha/\epsilon$  control and surface protection for solar cell arrays may be inadequate.

The energy lost in the conversion in solar cells of solar radiation to electrical power results principally from four factors: reflection; recombination; the forward leakage current through the converter; and the fact that the photon energy greater than that required to produce hole-electron pairs does not contribute to useful output.

Untreated silicon solar cells reflect about 10 percent of the incident sunlight in the wavelength range

# Non-Precision Capacitors

By ALBERT LUNCHICK,

Capacitor Development Unit, U. S. Army Signal Research and Development Laboratory, Fort Monmouth, N. J.

RAPID PROGRESS in capacitor development has produced a varied array of types and designs. This creates a situation where optimum choice of capacitors for a particular application could be overlooked.

Table I lists various types of electrolytic and general-purpose ceramic capacitors. These two categories are included in one tabulation because their broad tolerance makes them usable as by-pass or filter capacitors where bulk capacitance of guaranteed

minimum value is needed. These applications do not require the low dissipation factor, stability and high insulation resistance values found in precision and semiprecision capacitors.

The table includes those styles most likely to be encountered and does not preclude the use of less common or special types which are commercially available. The table lists only those parameters which permit ready comparison.

Table I—Nominal Characteristics of Electrolytic and General-Purpose Ceramic Capacitors (25 C)

	MIL Spec	MIL Style	Temp. Range Deg C	Volts D-C	Capacitance $\mu$ f	Insul. Res. Limit (Megohms)	Max. % Cap. Var. with Temp.	Diss. Factor Limits (%)	Polarized	Volumetric Eff. ( $\mu$ f/in. <sup>3</sup> )	Remarks
<b>Electrolytic</b>											
Aluminum	C-62	CE	-40 +85	15- 450	4-2,000	<3	+15 -75	15- 50	yes	5-450	Two-year shelf-life limit
Tantalum	C-3965	CL24	-55 +85	15- 150	1-580	0.5-30	+50 -40	15- 20	yes, no	55- 1,900	Etched foil, wet
Tantalum	C-3965	CL34	-55 +85	3- 150	0.5-300	0.2-40	+25 -45	15- 25	yes, no	25- 1,000	Plain foil, wet
Tantalum	C-3965	CL44	-55 +85	6- 125	2-60	6-40	+30 -50	4- 25	yes	75- 1,300	Wet, sintered anode
Tantalum	C-3965	CL15	-55 +175	18- 630	4-240	0.2-15	+40 -60	5- 45	yes	3- 600	Wet, sintered anode, double cased
Tantalum	C-55057 (Sig C)	CS12	-55 +85	6- 35	0.1-68	0.5-400	$\pm$ 10	3-6	yes	30- 6,000	Dry, sintered anode
Aluminum (axial leads)	6410 <sup>a</sup>		-40 +85	150- 450	5-20	<10	+15 -50	15	yes	35	High-purity foil, tubular can
<b>General-Purpose Ceramic</b>											
Ceramic <sup>a</sup>	C-11015	CK6	-55 +85	500	0.00047 0.01	>10,000	+30 -80	3	no	<0.2	Plate or disc
Ceramic <sup>a</sup>	C-11015	CK2	-55 +85	500	0.0001 0.0047	>10,000	+30 -80	3	no	<0.1	Tubular
Cerafil <sup>a</sup>	6407 <sup>b</sup>	CK1	-55 +85	100	0.001 0.047	>10,000	+10 -25	2.5	no	<4	Aerovox trade name
Stable <sup>a</sup>	6401 <sup>b</sup>	Char. X	-55 +85	500	0.00022 0.0047	>10,000	$\pm$ 15	1.5	no	<0.1	Plate, disc or tubular
Feed-through, Stand-off	6406 <sup>b</sup>	—	-55 +85	500	0.00047 0.002	>10,000	+30 -80	2	no	<0.1	High-frequency bypass
Monolythic <sup>a</sup>	—	—	-55 +85	25	0.075 0.75	>10,000	+30 -80	4	no	3-25	Sprague trade name
Ceramic <sup>a</sup>	—	—	-55 +85	75- 150	0.001 0.01	>10,000	+30 -80	3	no	<0.5	Plate or disc
Stable <sup>a</sup>	—	—	-55 +125	50	0.001 0.1	>10,000	+10 -15	2	no	15	Under development
Fluorinated <sup>a</sup>	—	—	-55 +200	50- 500	0.0001 0.01	>50,000 <sup>c</sup>	—	3	no	—	Proposed prod. development

(a) High dielectric constant (b) Signal Corps technical requirements (U. S. Army Signal Research and Development Lab). These spec numbers prefixed by SCL. (c) Insulation resistance limit >5,000 at 200 C

# Digital Control of Machine Tools

Thyratrons control a milling machine by driving step motors in response to signals from a programmed tape

By A. G. THOMAS, Charlottesville, Virginia

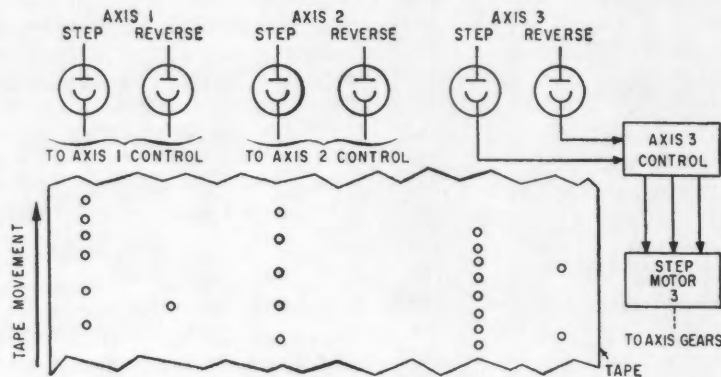


FIG. 1—Pictorial representation of system. Tape moves in plane between phototubes and a light source which is not shown

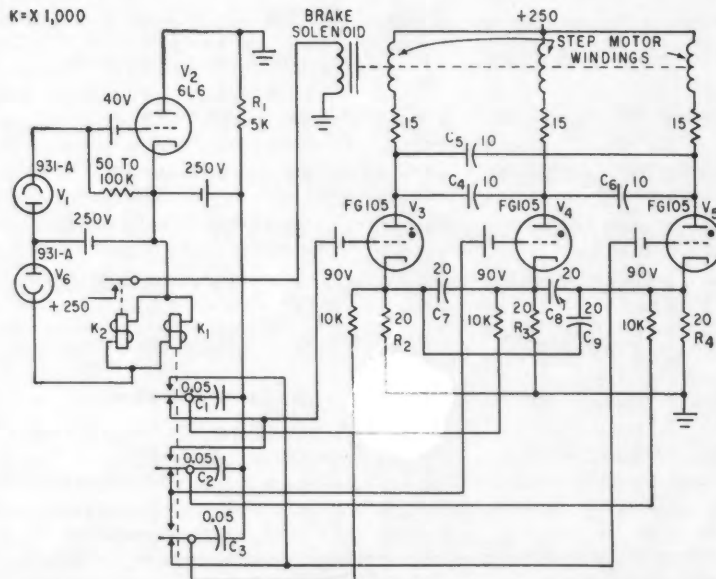


FIG. 2—These circuits control one step motor. The 1-Kv supply for phototubes  $V_1$  and  $V_6$  is not shown

**I**N THE SYSTEM to be described, three step motors drive the table, cross feed, and knee-elevating mechanism of a milling machine. These motors move one step at a time in response to pulses supplied by tape-controlled thyratrons.

## Overall Operation

Figure 1 gives a simplified picture of the system. Control information is in the form of punched holes in the tape. These holes modulate a light source (not shown in Fig. 1) which is directed to six phototubes.

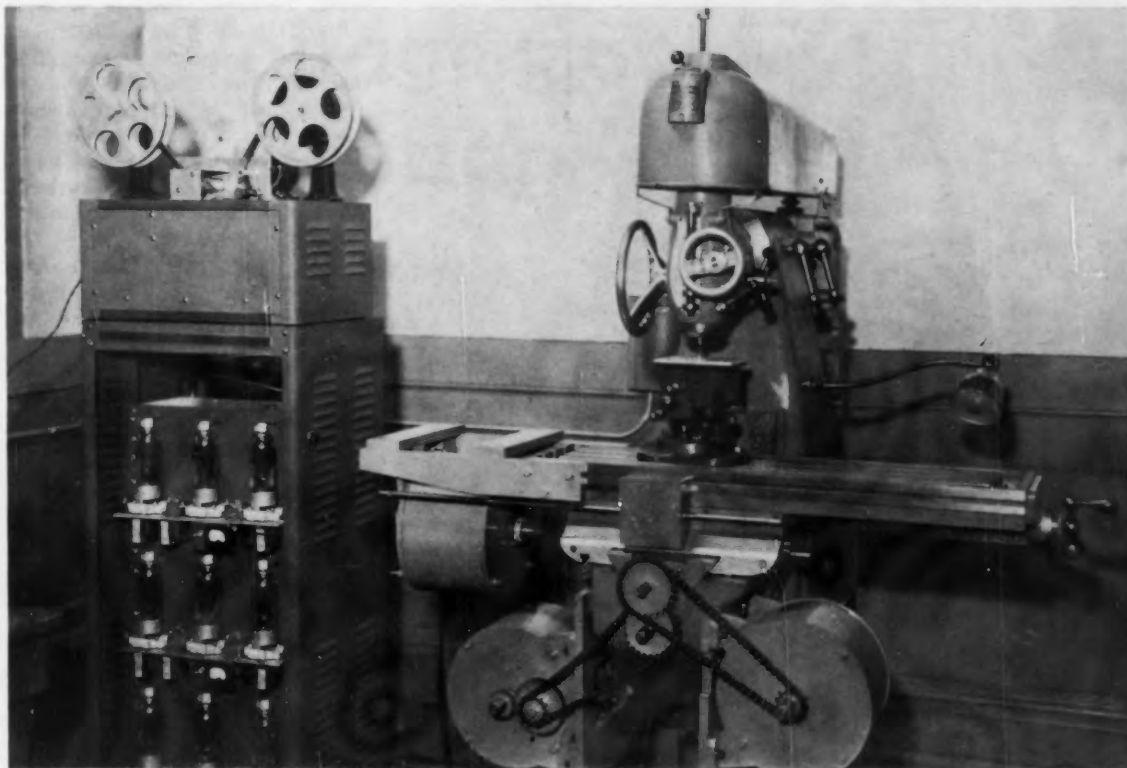
Each pair of phototubes controls movement in one of the three axes of movement of the milling machine. For example, consider movement in axis 3. Each light pulse to the STEP phototube of this axis pulses the axis 3 control circuit. This control circuit pulses step-motor 3, rotating it forward or backward over a discrete arc. Gearing transforms step-motor rotation into axis movement. Light passing through a reverse-signal hole pulses the REVERSE phototube, which signals a reversing circuit of axis 3 control; thus the step-signal hole following the reverse-signal hole steps the motor in the reverse direction.

Identical axis-control circuits, which are not shown in Fig. 1, produce movement in axes 1 and 2.

## Control Circuits

Each axis is controlled by a circuit identical to that shown in Fig.





The milling machine's electronic operator at the left gets its instructions from the tape above

2. This figure does not show the light source or the tape that modulates the light directed to phototubes  $V_1$  and  $V_2$ .

Phototube  $V_1$  is connected in the grid circuit of negatively-biased tube  $V_2$ . A step light pulse to  $V_1$  causes  $V_2$  to pass current through resistor  $R_1$ .

The voltage pulse across  $R_1$  passes through capacitances  $C_1$ ,  $C_2$  and  $C_3$ . The grids of thyratrons  $V_3$ ,  $V_4$  and  $V_5$  receive these pulses through the contacts of relay  $K_1$ .

These thyratrons are negatively biased, except for any thyatron which happens to be fired. Because of the cathode-connected resistors  $R_2$ ,  $R_3$  and  $R_4$ , and the tying of these resistors to the grids of other thyratrons, a conducting thyatron applies a positive potential to the grid of the thyatron that is next in the firing order, but without a sufficiently positive potential to fire it.

When the next step pulse from phototube  $V_1$  is applied to all the grids of the thyratrons, only the tube whose grid potential has been raised fires, since the firing pulses

are not sufficiently positive to overcome the full negative-bias potentials at the grids of the other thyratrons. Thus, successive pulsing of the grids of  $V_3$ ,  $V_4$  and  $V_5$  causes them to fire, sending successive pulses through the step-motor field windings.

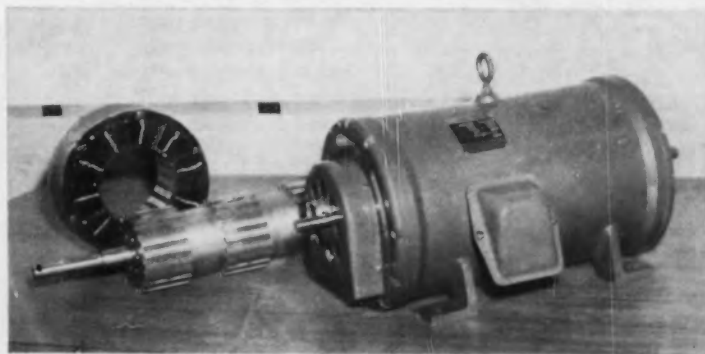
Capacitors  $C_1$ ,  $C_2$  and  $C_3$  quench the current of a thyatron when the next thyatron in the firing order fires. By using additional cathode-connected quenching capacitors  $C_4$ ,  $C_5$  and  $C_6$ , the capacitances of  $C_1$ ,  $C_2$

and  $C_3$  are considerably reduced. Thus harmful currents circulating through the motor windings are reduced and better speed and more stable operation are attained.

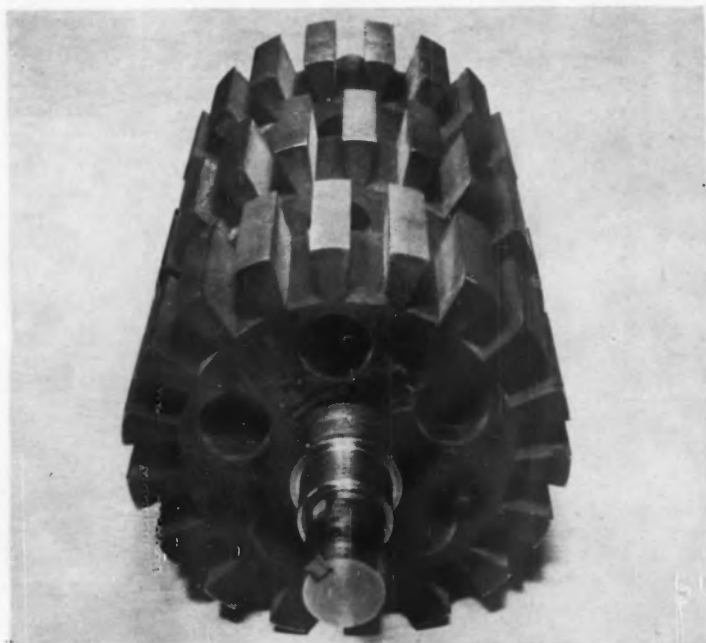
#### Reversing Rotation

Reversal of step-motor rotation occurs when a punched hole in the tape delivers a light pulse to phototube  $V_6$ . This tube passes current through relays  $K_1$  and  $K_2$ .

Relay  $K_2$  pulls in, energizing the brake solenoid, which prevents the



Disassembled step motor shows only one of the field windings



The rotor is essentially three rotors in one, all mounted on the same shaft and each displaced by a predetermined amount

step motor from moving in the direction opposite to the desired direction; before the solenoid is energized, the brake allows step-motor travel only in the forward direction.

When relay  $K_1$  pulls in, it switches the cathode connections of each tube so that firing order is reversed. For example, with  $K_1$  de-energized, and  $V_3$  conducting,  $V_3$  would be the next tube to fire; with  $K_1$  energized and  $V_3$  conducting,  $V_1$  is the next tube to fire.

### Step Motors

The step motor is the heart of the milling-machine control system and makes possible many sim-

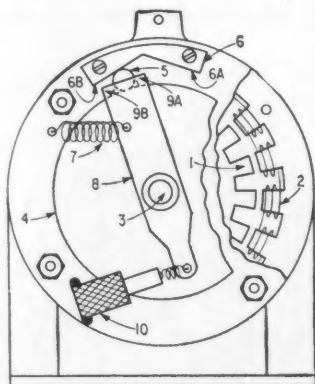


FIG. 3—Brake mechanism of step motor

plications. Early models of this motor were irregular in operation, sometimes suddenly jumping in the forward or reverse direction and at other times suddenly coming to a halt. These effects were due to the resilient magnetic system; as the field poles of the three sections (phases) were sequentially magnetized, the associated rotor poles would be strongly accelerated by magnetic attraction and would oscillate about the in-register position. That is, as the next field section was energized, the rotor might be travelling forward; the added forward pull might cause the rotor to jump several steps. Similarly, the rotor might be travelling backwards at the moment a field section was energized, so that the forces on the rotor would virtually cancel.

To solve this problem, a one-way locking device was attached to the motor and arranged to engage a brake disk at an appreciable radius from the axis of the shaft. This arrangement allows free rotation of the rotor in one direction but quickly locks the rotor against movement in the opposite direction. The reverse lock takes effect almost instantly at the greatest displaced position of the rotor, at which time its velocity is virtually

zero. Therefore braking is done without shock. The brake drums show no appreciable wear after many millions of steps.

Each field section has equally-spaced poles which are wound to produce alternate north and south poles when supplied with current.

The stators are set up so that the poles of the three sections are phased (staggered). That is, the arc covered by the trailing edges of the poles of one stator section is covered by the leading edges of the poles of another stator section. Rotor teeth, which are equally spaced so that they line up below stator poles, are in alignment from section to section.

Figure 3 shows a cutaway view of the motor. Part of a rotor section (1) and part of a stator section (2) are visible. Attached to the motor shaft (3) is a brake disk (4) which locks roller (5) against the hardened surface (6b) of cam (6) if the rotor tends to rotate in the counter-clockwise direction. Tension spring (7) normally holds arm (8) in the position shown. The rotor is free to rotate clockwise.

Roller (5) is caged between arms (9a) and (9b) which extend from bar (8). This bar is rotatable through a limited angle around the motor shaft (3).

When rotation of the motor is to be reversed, solenoid (10) is energized. The solenoid rotates bar (8) clockwise until roller (5) is pinched between disk (4) and cam surface (6a). The disk and rotor are then free to rotate in the counter-clockwise direction but are prevented from rotating in the clockwise direction. Consequently, the brake prevents oscillation of the rotor for both forward and reverse rotations.

### System Characteristics

Workpieces have been automatically milled for tolerances of 0.001 inch. No markings due to the step action are visible in the finished product. Movement per step can be set at any value desired by choosing the correct gear ratio but the finer the tolerance, the slower the workpiece movement. An electromechanical device encodes the signal-conveying information contained by the punched holes of the tape.

# Voltage-Controlled Bootstrap Generator

By combining a flip-flop and a bootstrap sweep generator, the output pulse length can be varied by a d-c bias or control voltage

By JOHN B. PAYNE III, Hughes Aircraft Company, Culver City, California

**P**HANTASTRON CIRCUITS are used to generate sweep signals, gating pulses and time delays. The circuits are popular because they are simple and reliable. Bootstrap sweep circuits can be made to generate the same type of waveforms as the phantastrons and they have a further advantage: the bootstrap circuits can be transistorized.

A typical phantastron circuit, such as that shown in Fig. 1, cannot be duplicated with any single transistor available today. The characteristics necessary for phantastron operation—sharp cutoff with both  $g_1$  and  $g_2$  grids—are available in such tubes as the 6AS6, 5915, etc., but not in transistors.

Definite savings in size, weight and power are realized when transistors are used in bootstrap circuits. The multipurpose bootstrap circuit uses a minimum number of transistors yet generates several waveforms. One output is a rectangular pulse or gate whose duration is directly proportional to the

level of the input control signal. A second waveform is a sweep with constant slope but controllable amplitude or duration. In addition, a highly linear sweep with a variable slope can be obtained.

## Circuit Operation

The basic circuit consists of a bootstrap sweep circuit coupled to a binary flip-flop, shown in Fig. 2A. The coupling is such that the binary is reset when the output sweep voltage reaches a specified level. This level  $V_A$  is variable, and thus the amplitude of the sweep can be changed. Because the slope of the output wave is not a function of the control voltage the duration of the wave is also controlled by this voltage. Since the gate output signal and the sweep signal are complementary, the duration of the gate is the same as the duration of the sweep, and thus controllable by  $V_A$ .

The basic bootstrap sweep circuit in Fig. 2A consists of transistor  $Q_3$  and its associated compo-

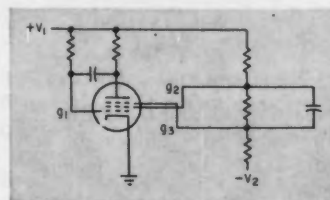


FIG. 1—Screen-coupled phantastron circuit supplies its own gate after being triggered

nents  $R_1$ ,  $R_2$ ,  $C_1$ ,  $C_2$  and  $D_1$ . The object of the circuit is to produce a constant charging current to  $C_1$ , thereby producing a linear rise in voltage. At the beginning of the sweep,  $Q_2$  is saturated, the charge on  $C_1$  is zero, the emitter-to-ground voltage of  $Q_3$  is zero and  $C_2$  is charged up to  $V_{cc}$ . Capacitor  $C_2$  has to be large compared to  $C_1$ , such that it loses very little of its charge during the sweep period. Operation of the circuit is such that  $C_2$  can be considered to be a battery.

As the voltage across  $C_1$  rises, the emitter voltage of  $Q_3$  increases by

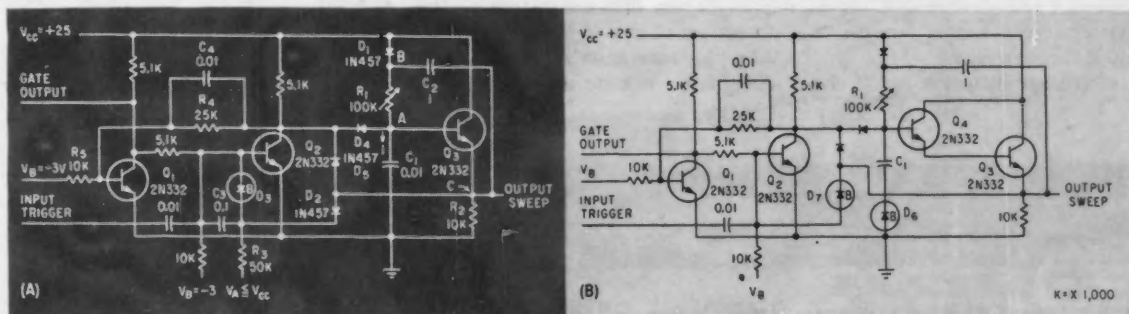


FIG. 2—Bootstrap circuit is coupled with flip-flop to give variable, controllable sweep (A). A highly linear version of the circuit has constant amplitude output and uses an extra transistor in the Darlington connection (B)

the same amount, since the voltage gain is almost unity. Because the charge on  $C_1$  changes very little, the voltage across  $C_2$  changes very little and the voltage at point  $B$  rises by the same amount as the voltage at point  $C$ . Point  $B$  therefore rises above  $V_{cc}$  but diode  $D_1$  blocks current flow to  $V_{cc}$ . Since points  $A$ ,  $B$  and  $C$  all rise in voltage by the same amount, the voltage drop across  $R_1$  is constant; therefore charging current to  $C_1$  remains constant and output voltage rises linearly.

The charging current will not be exactly constant because of secondary effects; the base current to  $Q_2$  changes slightly, the emitter-follower gain is not exactly unity, and  $C_1$  does lose a little charge. All these effects are small.

### Flip-Flop

Transistors  $Q_1$  and  $Q_2$  of Fig. 2A are connected as a binary flip-flop with  $D_2$ ,  $D_3$ ,  $R_3$ , and  $C_2$  as feedback for self-gating.

Prior to any trigger pulse,  $Q_2$  is saturated, with its collector voltage approximately zero. Diode  $D_1$  acts to discharge  $C_1$  and clamp it to ground potential;  $Q_1$  is biased to cutoff through the voltage divider formed by  $R_1$ - $R_2$  and its collector voltage is high, thus holding  $Q_2$  saturated. Voltage  $V_A$  holds  $Q_1$  cut off. At room temperature, the voltage  $V_B$  and resistors  $R_1$  and  $R_2$  can be eliminated; they are required at high temperatures, however. If silicon transistors are used, the hold-off circuits can be eliminated even at high temperature.

The circuit is triggered by a negative pulse arriving at the base of  $Q_2$ , driving this transistor to cutoff and throwing  $Q_1$  into saturation, with  $C_1$  acting as a speed-up capacitor. The collector of  $Q_2$  rises,  $D_1$  is back-biased and the top of  $C_1$  is no longer grounded but is free to be charged through  $R_1$ .

The voltage drop across  $R_2$  in-

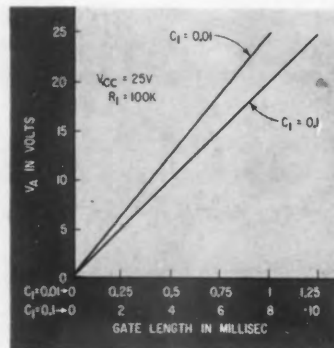


FIG. 3—The length of the gate is varied over a large span by controlling the bias voltage

### EQUATIONS OF SWEEP TIMING CIRCUIT

The voltage across  $C_1$  is given by

$$V_{C1} = \frac{1}{C_1} \int_0^t idt \quad (1)$$

$$\text{where } i = \frac{V_{cc}}{R_1} \quad (2)$$

The rate of change of voltage across  $C_1$  is

$$\begin{aligned} \frac{dV_{C1}}{dt} &= \frac{d}{dt} \left[ \frac{1}{C_1} \int_0^t idt \right] \\ &= \frac{i}{C_1} \text{ (volts/sec)} \end{aligned}$$

$$\text{or } \frac{dV_{C1}}{dt} = \frac{V_{cc}}{R_1 C_1} \quad (3)$$

The slope of the output sweep is  $V_{cc}/R_1 C_1$  in volts per second; sweep amplitude is  $V_A$ ; gate time, which is also the duration of the sweep is  $R_1 C_1 V_A / V_{cc}$ .

increases linearly until the sweep voltage reaches  $V_A$ , at which time  $D_2$  is forward biased, driving the base of  $Q_2$  positive. Zener diode  $D_3$  is shunted across  $C_2$  to insure that  $Q_2$  is driven into saturation if the charge on  $C_2$  should become greater than the maximum sweep voltage. The Zener voltage should be less

than  $V_{cc}$  but at least as large as the maximum sweep amplitude required. As soon as  $Q_2$  starts to conduct, the flip-flop will return to its initial conditions, in which the collector voltage of  $Q_2$  goes to zero and discharges  $C_1$  through  $D_1$ . Diode  $D_2$  provides a low impedance path to ground for  $C_2$  to recharge quickly to  $V_{cc}$ . The bootstrap sweep circuit is much less sensitive to changes in repetition rate because of the path provided by  $D_2$ .

### Circuit Waveforms

By varying  $V_A$ , the sweep and gate lengths can easily be changed. The circuit of Fig. 2A was tested for various values of  $V_A$  to determine the effect on gate length, with the results shown in Fig. 3. Waveforms for two different values of  $V_A$  are shown in Fig. 4A and 4B, which show both the gate and the ramp functions.

Although the linearity is extremely good, as is shown in more detail in Fig. 4C, it can be improved further by adding another transistor to  $Q_2$  in the Darlington connection, as is done in the circuit of Fig. 2B. The linearity that this extra transistor gives is shown in Fig. 4D, which can be compared with Fig. 4C by sighting along the page or by comparing with a straight edge.

A pedestal on the sweep, as in Fig. 4E, can be obtained by adding a Zener diode between  $C_1$  and ground, as  $D_4$  in Fig. 2B. The amplitude of the pedestal will be equal to the Zener voltage.

If a fixed sweep amplitude is desired, the circuit can be simplified somewhat. Thus Fig. 2A is simplified by replacing  $D_2$ ,  $D_3$ ,  $C_2$ ,  $R_3$ , and  $V_A$  by Zener diode  $D_7$ , as in Fig. 2B.

### REFERENCES

- (1) J. Millman and H. Taub, "Pulse and Digital Circuits", p. 222, McGraw-Hill Book Company, N. Y., 1956.
- (2) Chance, Britton, et al., "Waveforms," MIT Radiation Series, 19, McGraw-Hill Book Company, N. Y. 1949.

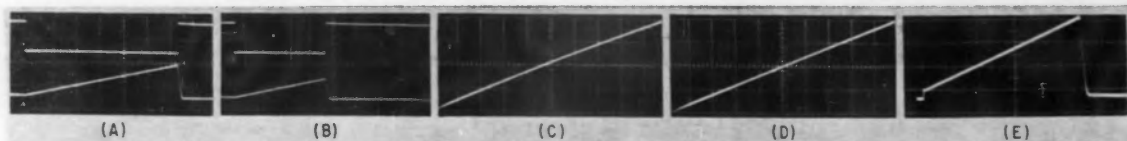


FIG. 4—Waveforms of the bootstrap generator. (A) and (B) show the effect of the control voltage  $V_A$  on the gate and ramp outputs. (C) is an enlargement of the ramp of Fig. 2A, (D) for Fig. 2B, showing the increase in linearity obtained from the Darlington connection. Ramp function on a pedestal is shown in (E)